Sustainable Materials and Technologies 43 (2025) e01215

Contents lists available at ScienceDirect

Sustainable Materials and Technologies

journal homepage: www.elsevier.com/locate/susmat

Rapid and efficient dehydration of cellulose nanofiber hydrogels via electroosmosis

Takaaki Kasuga *, Ami Mizui, Shun Ishioka, Hirotaka Koga, Masaya Nogi

SANKEN (The Institute of Scientific and Industrial Research), Osaka University, Ibaraki, Osaka 567-0047, Japan

ARTICLE INFO

Keywords:
Cellulose nanofibers
Nanocellulose
Electroosmosis
Dehydration
Transparent film

ABSTRACT

Efficient dehydration of cellulose nanofiber (CNF)/water dispersions and hydrogels is still a challenge in the industrial use of CNFs. In this study, electroosmosis of CNF hydrogels was evaluated as a dehydration method. TEMPO-oxidized CNF hydrogels were rapidly dehydrated by applying DC 20 V, and the CNF concentration increased from 0.5 wt% to ~10 wt% within 3 min. The energy efficiency of dehydration was more than 7 times greater than that of evaporation, and the resulting concentrated CNF hydrogels were successfully redispersed through a simple neutralization process. In addition, the anisotropic shrinkage of CNF hydrogels due to electroosmosis is suitable for CNF film preparation. This work provides new insights into dehydration methods for CNF/water dispersions and hydrogels.

1. Introduction

In order to realize a sustainable society, there is a need to use biomass in various fields, such as the development of functional materials [1–5]. In particular, cellulose nanofibers (CNFs) are promising biomass-derived nanomaterials with excellent properties, such as light weight, high strength, transparency, thermal resistance and sustainability [6–8]. CNFs are expected to be used for various applications, including functional films, filters, composites, and dispersion stabilizers [9–13]. In particular, CNFs with widths of ~3 nm, such as TEMPO-oxidized CNFs, are expected to be fundamental materials for sophisticated functional materials because of their large specific surface area, suitability for surface modification, and transparency [6,10,12,13]. However, the industrial use of CNFs is still limited to a few areas. One of the technical hindrances to industrial use is the dehydration of CNF/water dispersions [14]. CNFs are prepared as dilute water dispersions from wood pulps or other resources [6–8]. The concentration of CNF/water dispersions is typically less than 2 wt%, with more than 98 wt% water. The use of such dilute dispersions entails enormous storage and transportation costs. Moreover, additional energy and time are required for dehydration to prepare dried CNF products such as films, filters and molds.

Various methods to improve the efficiency of the dehydration process have been reported, including filtration, evaporation, osmotic concentration and freeze–thaw cycling [9,10,14–18]. High-efficiency rapid dehydration of CNF/water dispersions to higher concentrations is still difficult because of the high affinity for water and high surface area of CNFs. In recent years, electrodeposition has received much attention as an effective dehydration method for nanocellulose [19–23]. During electrodeposition, hydrogelation of CNFs via electrochemical reactions and dehydration via electroosmosis enable highly efficient dehydration of dilute CNF/water dispersions. As a disadvantage of electrodeposition, increasing the concentration of the CNF/water dispersion to higher than 2 wt% takes time [23]. In addition, dehydration to high concentrations (e.g., ~10 wt%) is difficult. The dehydration process must be improved to reduce the dehydration time and increase the CNF concentration.

Electroosmotic dehydration is known as an efficient dehydration method for particulate dispersions [24–26]. It is an electrokinetic approach for dehydration that uses electroosmosis and has been developed mainly as a dewatering technology for sludge [25]. Electroosmotic dehydration is performed by applying a voltage to the dehydration target (e.g., sludge), which is a mixture of a solid and a liquid (water). In water, adsorbed or dissociated ions form an electric double layer on the solid surface. When a voltage is applied in this state, movement of the ions in the electric double layer is induced by the electric field between the electrodes, and hydrated water molecules move with the moving ions, generating a water flow called electroosmotic flow. The solid particles are fixed by a filter or another method, and the water is extruded from the dehydration target by the electroosmotic flow [25].

* Corresponding author.
E-mail address: tkasuga@eco.sanken.osaka-u.ac.jp (T. Kasuga).

https://doi.org/10.1016/j.susmat.2024.e01215
Received 19 November 2024; Received in revised form 6 December 2024; Accepted 8 December 2024
Available online 10 December 2024

The filtration and mechanical compression methods normally used for dehydration require a long time to dehydrate sludge-like particle dispersions [23–25]. On the other hand, electroosmotic dehydration is limited to charged particles, however, it is faster than filtration and consumes less energy than thermal dehydration. The surface charge density of the solid particles is an important factor for the generation of electroosmotic flow. Therefore, TEMPO-oxidized CNFs with a high surface charge density are likely suitable for electroosmotic dehydration.

Herein, we report a fast and efficient dehydration method for CNF hydrogels via electroosmosis to overcome the trade-off between time and energy consumption during dehydration and accelerate the industrial use of CNFs. Our method targeted CNF hydrogels instead of CNF/water dispersions and achieved rapid dehydration and simplified dehydration equipment. In addition, we propose a dehydration strategy that combines electrodeposition and electroosmosis dehydration, which can be applied to CNF/water dispersions as starting materials. The anisotropic shrinkage caused by electroosmotic dehydration could be applied to CNF film preparation. The findings of this study will accelerate the industrial use of CNFs.

2. Methods

2.1. Materials

1 M hydrochloric acid solution and 0.1 M sodium hydroxide aqueous solution were purchased from Nacalai Tesque, Inc. (Japan). TEMPO-oxidized cellulose pulp (carboxylate content: 1.8 mmol/g) was supplied by DKS Co., Ltd.

2.2. Preparation of CNF/water dispersions and CNF hydrogels

The 0.6 wt% TEMPO-oxidized cellulose pulp slurry was homogenized by a high-pressure water-jet system (HJP-25008, Sugino Machine Co., Ltd., Japan) equipped with a ball-collision chamber. The slurry was passed through a small nozzle (diameter: 0.15 mm) under a pressure of 200 MPa 5 times. The resulting dispersion was adjusted to a concentration of 0.5 wt% for subsequent use. The 0.5 wt% CNF aqueous dispersions along with molds (diameter: 20 mm or 30 mm, thickness: 10 mm) were immersed in 1 M hydrochloric acid for 3 h. The resulting H-type CNF hydrogels were thoroughly washed with distilled water to remove excess hydrochloric acid.

2.3. Electroosmotic dehydration

Two 50 × 50 × 0.1 mm platinum electrodes were used for electroosmotic dehydration. The CNF hydrogels were sandwiched between the upper (anode) and lower (cathode) electrodes, and a load of 1 N (pressure: ~3.2 mN/mm^2) was applied to ensure constant contact with the electrodes. Voltages ranging from 5 to 20 V were applied by a source measurement unit (B2902A, Keysight Technologies, USA). After voltage application for 1–5 min, the CNF hydrogels were collected, and the CNF concentration was quantified by drying the samples at 110 °C.

2.4. Redispersibility test

Hydrogelation and predehydration via electrodeposition were carried out according to the same procedure as previously reported [23]. The CNF/water dispersions were adjusted to a concentration of 0.2 wt% for electrodeposition. Two 100 × 100 × 5 mm graphite electrodes were placed in an acrylic cell (with a distance of 3 cm between the electrodes), and the cell was filled with 2 L of a 0.2 wt% CNF/water dispersion. DC 5 V was applied between the electrodes by a source measurement unit (B2902A, Keysight Technologies, USA) for 1 h. The obtained CNF hydrogels (~1.2 wt%) were collected and concentrated via electroosmotic dehydration at DC 20 V for 3 min to obtain highly concentrated CNF hydrogels (~13.5 wt%). For neutralization, the CNF hydrogels were diluted to 0.5 wt%, and a 0.1 M sodium hydroxide solution was added to the redispersed CNF dispersion until the pH of the dispersion reached 7. For redispersion, the CNF dispersions were diluted to 0.2 wt% by adding distilled water and homogenized at 8000 rpm for 10 min with a homogenizing mixer (MARKII Model 2.5, PRIMIX Corp., Japan). The transmittances of the CNF/water dispersions were measured with a UV–vis–NIR spectrophotometer (UV-3600 Plus, Shimadzu Corp., Japan). Fourier transform infrared (FT-IR) spectra and X-ray diffraction (XRD) patterns of CNF films prepared by drying the original and redispersed CNF/water dispersions were obtained with an FT-IR spectrometer (Frontier TN, PerkinElmer Inc., USA) and a desktop X-ray diffractometer (MiniFlex600, Rigaku, Japan) with Cu Kα radiation over a scanning angle (2θ) range of 5–45° at a 40 kV voltage and a 15 mA current.

3. Results

3.1. Electroosmotic dehydration of CNF hydrogels

0.5 wt% Cylindrical CNF hydrogels were sandwiched between platinum electrodes on top and on bottom, and 5–20 V was applied (Fig. 1a). In this study, platinum electrodes were used to prevent contamination by anodic metal ions and products during electroosmosis [27,28]. When 20 V was applied, the hydrogel thickness decreased from 10 mm to less than 1 mm within 3 min. The CNF concentration of the concentrated CNF hydrogels increased to ~10.2 wt% (Fig. 1b-d). This result indicated that more than 95 % of the water in the hydrogel was dehydrated within 3 min, and the CNF concentration increased to 20 times greater than the original value. The dehydration was faster under a higher voltage, and the CNF concentration increased with a longer voltage application time (Fig. 1d). Unlike dehydration via evaporation, in electroosmotic dehydration, the dehydrated water was extruded from the hydrogel as water, not water vapor (Supporting Video S1). The water was expelled from the interface between the upper cathode and the hydrogel. In electroosmotic dehydration, dehydration proceeds via electroosmotic flow [25]. In this case, protons (H+) generated by electrolysis of water at the anode migrated to the cathode, causing electroosmotic flow inside the CNF hydrogel, and water was discharged from the cathode side.

3.2. Comparison of the dehydration energy efficiencies for evaporative dehydration and electroosmotic dehydration

Next, the efficiency of CNF hydrogel dehydration via electroosmotic dehydration was calculated. The dehydration efficiency was defined as the ratio of the amount of dehydrated water [g] to the amount of energy consumed [Wh] [23,25]. Dehydration of the 0.5 wt% CNF hydrogel to 10 wt% by applying 20 V for 3 min was ~7 times more efficient than evaporative dehydration (Fig. 2). Electroosmotic dehydration removes the water inside the hydrogel as water, rather than water vapor, as in vacuum filtration [29] and osmotic dehydration [16]. Therefore, less energy is required than in evaporative dehydration. As dehydration progresses and the solid concentration of the hydrogel increases, the energy consumption tends to increase (Fig. 3). The efficiency of electroosmotic dehydration has been reported to gradually decrease as dehydration progresses [26]. The reasons for the decrease in the dehydration efficiency include a decrease in the pH inside the dehydration target and ionic conduction inhibition due to the high concentration of particles around the anode [25]. There was no significant difference in the efficiency with the different applied voltages in this study, and it was confirmed that the final CNF concentration tended to determine the efficiency (Fig. 3). This result suggests that for dehydration up to 10 wt %, the approach of high voltage (e.g., 20 V) application and rapid dehydration may be effective.

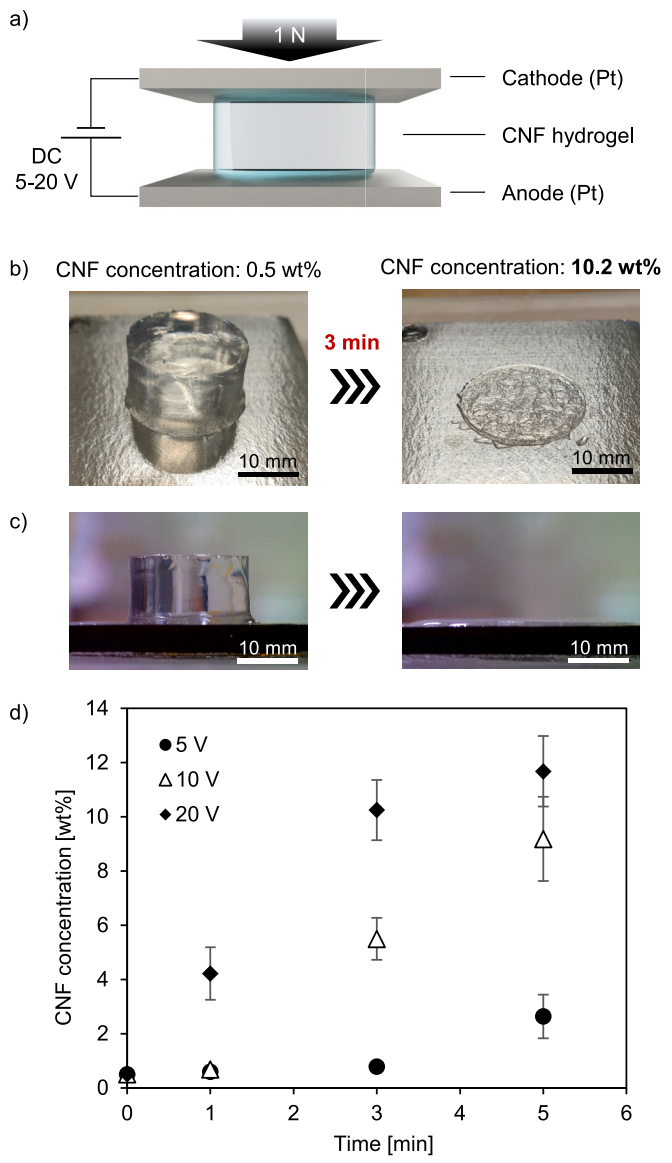

Fig. 1. a) Outline of the electroosmotic dehydration system. b) Overhead view and c) side view of CNF hydrogel before and after dehydration. d) CNF concentration in CNF hydrogels after electroosmotic dehydration realized by applying DC 5–20 V for 1–5 min.

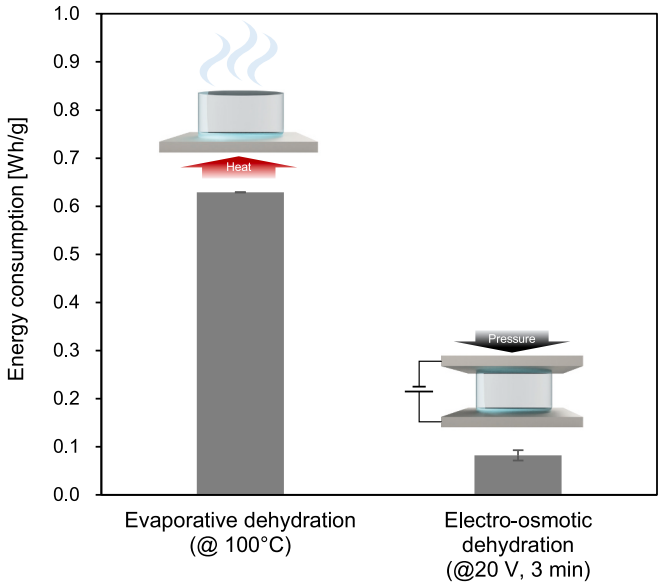

Fig. 2. Comparison of the energies consumed by evaporation and electrodeposition for dehydration from 0.5 wt% to ~10 wt%.

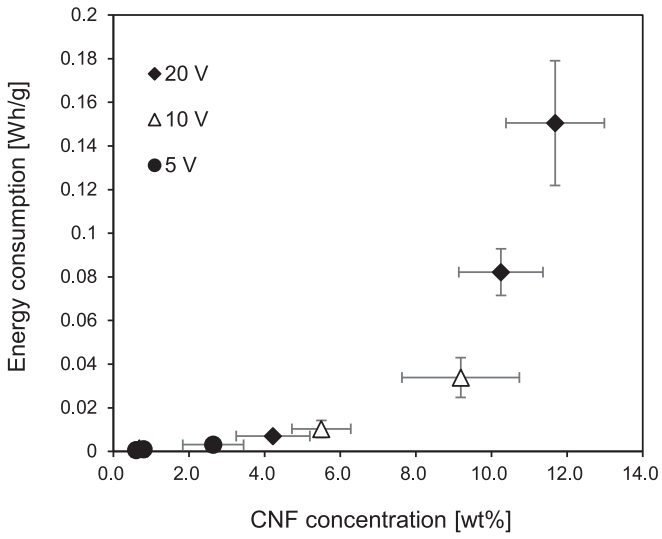

Fig. 3. Energy consumption relative to the concentration of CNFs after electroosmotic dehydration.

3.3. Dehydration and redispersion strategy

In this study, electroosmotic dehydration was applied to H-type TEMPO-oxidized CNF hydrogels [30,31]. The hydrogels were prepared by immersing Na-type TEMPO-oxidized CNF/water dispersions in hydrochloric acid. Under low pH conditions such as hydrochloric acid, the counter ions of the carboxy groups on the surface of CNFs are converted from Na^+ to H^+, and CNFs partially aggregate and form a hydrogel [30]. However, gelation using hydrochloric acid is not desirable in industry because it involves additional washing processes and the discharge of waste liquid. On the other hand, electrodeposition-based hydrogelation can be used to directly prepare H-type TEMPO-oxidized CNF hydrogels from industrially produced Na-type TEMPO-oxidized CNFs without additional washing processes [23,32]. Therefore, we evaluated a dehydration strategy that combines electrodeposition and electroosmotic dehydration, targeting individually dispersed Na-type TEMPO-oxidized CNFs (Fig. 4a). First, electrodeposition was applied to 0.2 wt% CNF/water dispersions [23]. After electrodeposition at DC 5 V for 1 h, H-type TEMPO-oxidized CNF hydrogels (~1.2 wt%) were obtained. The obtained CNF hydrogels were electroosmotically dehydrated at DC 20 V for 3 min to obtain highly concentrated CNF hydrogels (~13.5 wt%). In this process, the starting materials, 0.2 wt% CNF/water dispersions, were converted into ~13.5 wt% CNF hydrogels. More than 95 wt% of the water in the original dispersion was removed with high energy efficiency. Next, the effects of electroosmotic dehydration on CNFs were evaluated. The highly concentrated CNF hydrogels were neutralized by NaOH, redispersed and then compared with the original dispersions. The appearance of the CNF/water dispersion after dehydration and neutralization process was the almost same as before dehydration (Fig. 4a). FT-IR measurements revealed no significant change in the chemical structure of the CNFs after dehydration (Fig. 4b). In addition, no significant change was observed in the crystal structure of the CNFs (Fig. 4c). The results suggest that there are no significant inter-crystal interactions that have a strong effect on the redispersion of CNFs [40–42]. However, the transmittance of the redispersed CNF/water dispersion was slightly lower than that of the original dispersion

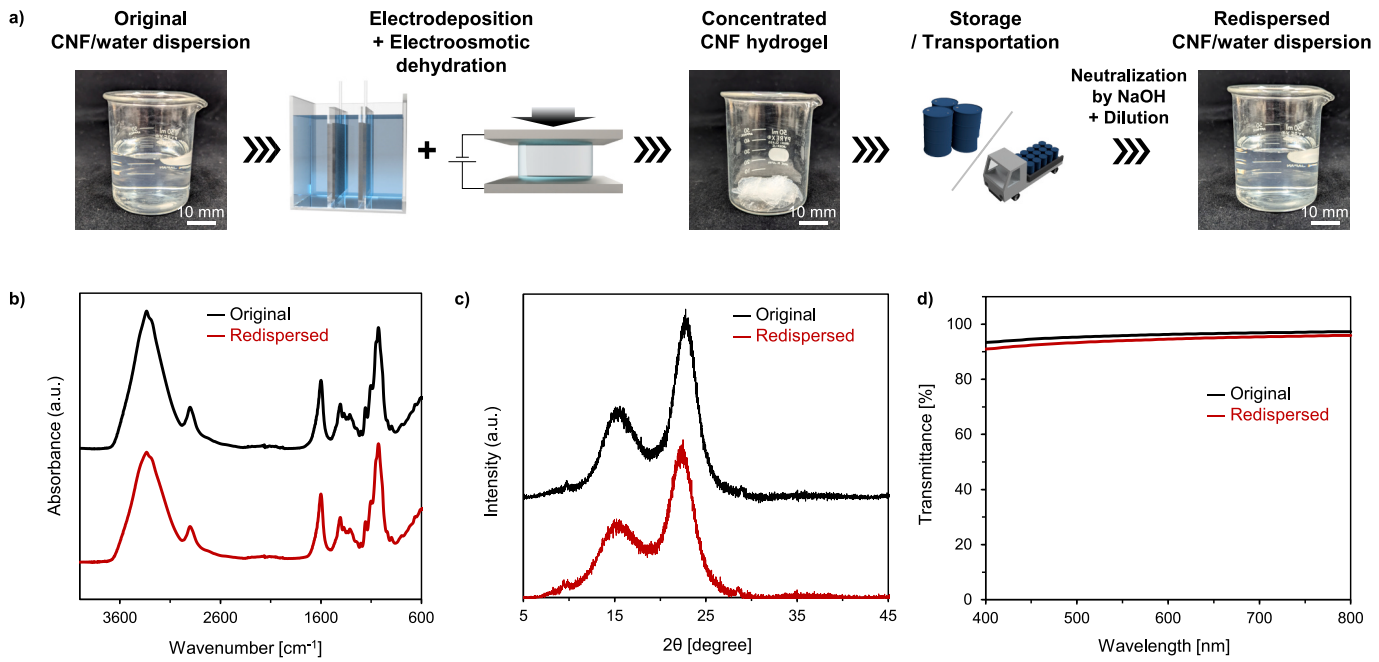

Fig. 4. a) Storage/transportation/redespersion strategy for CNFs via electrodeposition and electroosmotic dehydration. b) FT-IR spectrum, c) XRD pattern and d) transmittance of the original and redispersed CNF water dispersions.

(Fig. 4d). These results suggested that small CNF aggregates remained in the redispersed CNF/water dispersion [26–28]. When the concentration was increased to around 1.6 wt% by electrodeposition, the transparency of the dispersion did not change [23], therefore, these small CNF aggregates were formed during electroosmotic dehydration. Such CNF aggregates might cause a decrease in the performance of CNF films and changes in the viscosity of the dispersion [23,33–35,42]. In the future, it is necessary to optimize the electroosmosis conditions and disintegrate the aggregates through additional homogenization. These results show that CNFs maintain almost the same properties as the original state even after electrodeposition and electroosmotic dehydration and that this strategy is promising as a rapid high-efficiency dehydration method.

3.4. Application of electroosmotic dehydration to film preparation

In the case of evaporative dehydration, water evaporates from all the interfaces between air and the CNF hydrogel. The hydrogel isotropically shrinks to a certain extent, and eventually, the dried product takes on a complex shape that reflects the orientation of the internal CNFs and differences in the drying speed (Fig. 5a) [22,36,37]. In the case of electroosmotic dehydration, water is expelled from the interface between the cathode and the CNF hydrogel because of the electroosmotic flow caused by the protons moving from the anode to the cathode (Fig. 5b) [25]. As a result, the CNF hydrogels anisotropically shrink, and sheet-like CNF hydrogels are obtained. The sheet-like CNF hydrogels are highly concentrated, and CNF films can be obtained via a short-term hot-pressing process (Fig. 6a). Compared with conventional film preparation methods such as dry casting and filtration, this method has advantages in terms of energy consumption and drying time. In addition, we successfully preparing thick CNF films using thick CNF hydrogels (Fig. 6b). When preparing thick CNF films of over 100 μm in size using individually dispersed CNFs such as TEMPO-oxidized CNFs, special techniques such as layering must be used due to problems with the drying time and complex drying shrinkage [38,39]. Electroosmotic dehydration enables easy preparation of thick CNF films because of its rapid dehydration and anisotropic shrinkage.

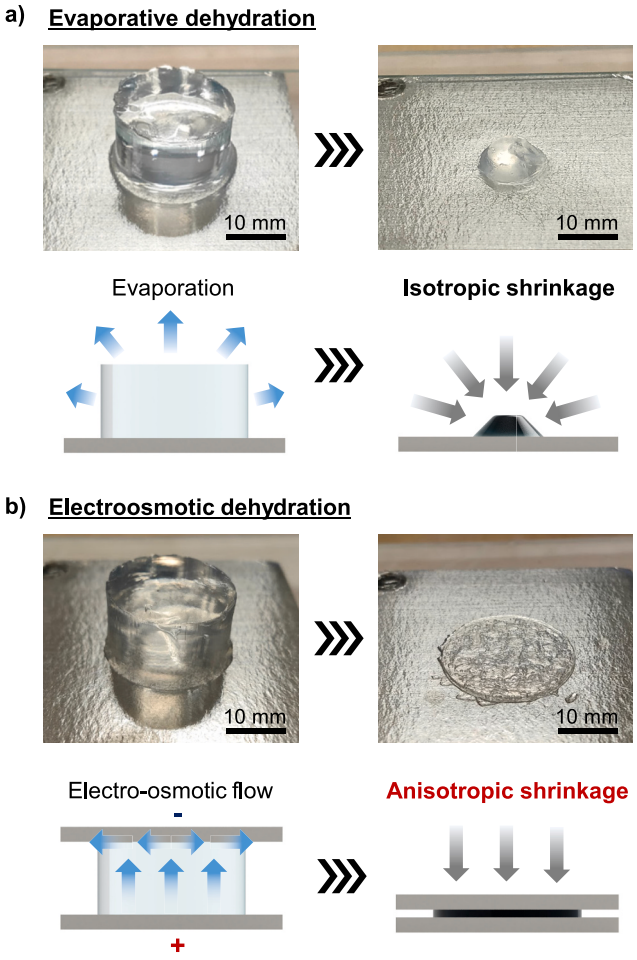

Fig. 5. a) Evaporative and b) electroosmotic dehydration processes of CNF hydrogels.

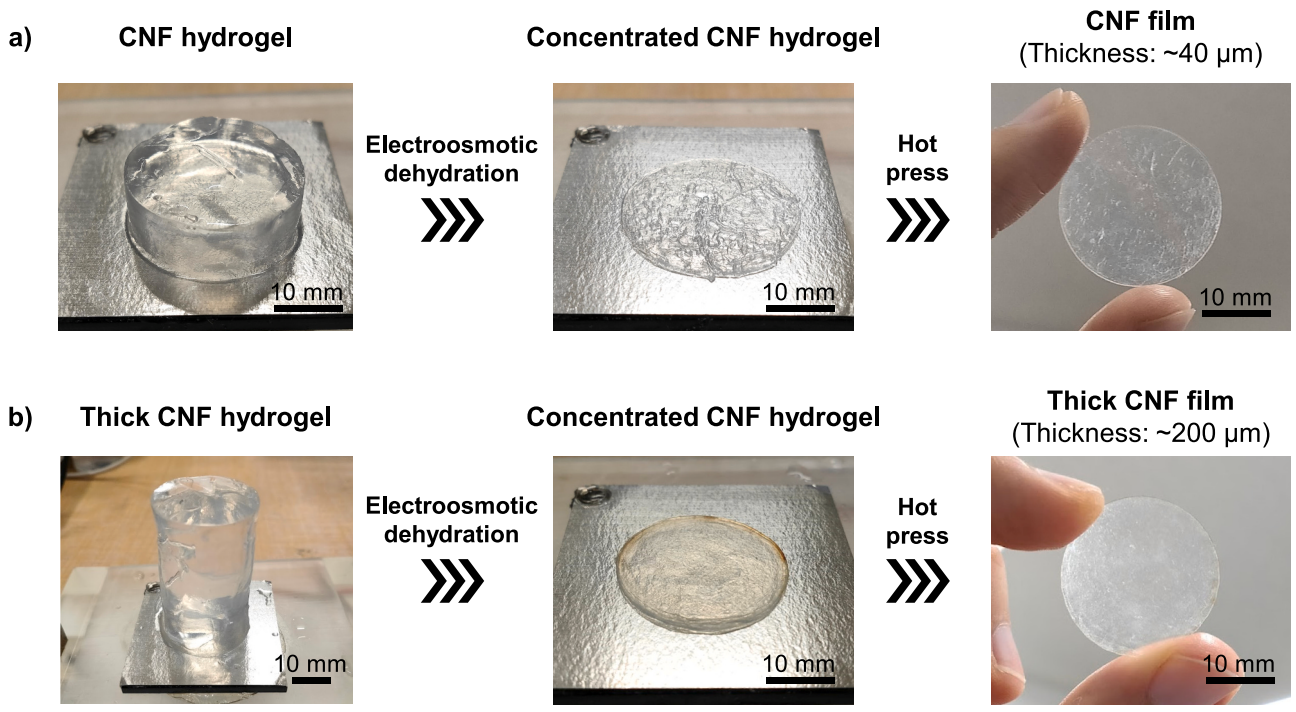

Fig. 6. a) Application of electroosmotic dehydration to film preparation. b) Thick CNF films can be prepared via a simple process that combines electroosmotic dehydration and hot pressing.

4. Conclusion

In summary, we evaluated electroosmosis of CNF hydrogels as a novel dehydration method. The electroosmotic dehydration of CNF hydrogels is fast, and concentrated CNF hydrogels can be redispersed as CNF/water dispersions through a simple neutralization process. By combining electrodeposition and electroosmotic dehydration, the CNF/water dispersions can be dehydrated with high efficiency. In addition, anisotropic shrinkage due to electroosmosis is suitable for preparing CNF films. Notably, electroosmotic dehydration is effective for individually dispersed CNFs with a high surface charge; however, it might have limited effectiveness for CNFs that do not have these characteristics (e.g., mechanically fibrillated CNFs). This research has succeeded in simplifying the dehydration equipment by using CNF hydrogel as the dehydration target. However, in order to use CNF/water dispersion as the starting material, it is essential to combine electrodeposition and electroosmotic dehydration, therefore, it is essential to develop a novel dehydration device that integrates these two processes to enable long-term operation in the future. In addition, further research is needed regarding the application in CNF film preparation, such as examination of the optimal voltage conditions and achievement of continuous film preparation. These results provide a new dehydration strategy for individually dispersed CNFs, which are particularly difficult to dehydrate.

Supplementary data to this article can be found online at https://doi.org/10.1016/j.susmat.2024.e01215.

Author statement

T. K was responsible for the conceptualization, methodology, investigation, writing - original draft, supervision, project administration and funding acquisition. A. M contributed for validation and data curation. S.I., H. K and M. N were responsible for validation, resources, and writing - review & editing. All authors have provided feedback and endorse the final version of the manuscript.

Funding

This work was partially supported by Grants-in-Aid for Scientific Research (Grant Numbers 22 K20592 and 24H00524), JST PREST (Grant Number JPMJPR24L6), JST CREST (Grant Number JPMJCR22L3), and the Shorai Foundation for Science and Technology.

CRediT authorship contribution statement

Takaaki Kasuga: Writing – review & editing, Writing – original draft, Visualization, Validation, Supervision, Resources, Project administration, Methodology, Investigation, Funding acquisition, Formal analysis, Data curation, Conceptualization. **Ami Mizui:** Investigation, Data curation. **Shun Ishioka:** Writing – review & editing, Project administration, Data curation. **Hirotaka Koga:** Writing – review & editing, Project administration. **Masaya Nogi:** Writing – review & editing, Project administration.

Declaration of competing interest

There are no conflicts of interest to declare.

Acknowledgements

This work was partially supported by Grants-in-Aid for Scientific Research (Grant Numbers 22K20592 and 24H00524), JST PREST (Grant Number JPMJPR24L6), JST CREST (Grant Number JPMJCR22L3), and the Shorai Foundation for Science and Technology.

Data availability

Data will be made available on request.

References

[1] K. Jin, Y. Tang, J. Liu, J. Wang, C. Ye, Nanofibrillated cellulose as coating agent for food packaging paper, Int. J. Biol. Macromol. 168 (2021) 331–338, https://doi.org/10.1016/J.IJBIOMAC.2020.12.066.

[2] B. Azimi, S. Sepahvand, S. Ismaeilimoghadam, H. Kargarzadeh, A. Ashori, M. Jonoobi, S. Danti, Application of Cellulose-Based Materials as Water Purification Filters; A State-of-the-Art Review, J. Polym. Environ. 32 (2023) 345–366, https://doi.org/10.1007/S10924-023-02989-6.

[3] Y. Ci, D. Lv, X. Yang, H. Du, Y. Tang, High-performance cellulose/thermoplastic polyurethane composites enabled by interaction-modulated cellulose regeneration, Carbohydr. Polym. 346 (2024) 122611, https://doi.org/10.1016/J.CARBPOL.2024.122611.

[4] S. Sadat Fazel, M. Jonoobi, K. Pourtahmasi, S. Sepahvand, A. Ashori, Enhancing the oil adsorption properties of cellulose nanofiber aerogels through chemical modification, J. Polym. Environ. 32 (2024) 1304–1313, https://doi.org/10.1007/s10924-023-03037-z.

[5] A. Haghighi Poshtiri, S. Sepahvand, M. Jonoobi, A. Ashori, A.N. Karimi, F. Hasanzadeh Fard, L. Bergamonti, C. Graiff, S. Palanti, Functionalized cellulose nanocrystals for enhanced wood protection: synthesis, characterization, and performance, Ind. Crop. Prod. 222 (2024) 120021, https://doi.org/10.1016/J.INDCROP.2024.120021.

[6] T. Saito, S. Kimura, Y. Nishiyama, A. Isogai, Cellulose nanofibers prepared by TEMPO-mediated oxidation of native cellulose, Biomacromolecules 8 (2007) 2485–2491, https://doi.org/10.1021/bm0703970.

[7] K. Abe, S. Iwamoto, H. Yano, Obtaining cellulose nanofibers with a uniform width of 15 nm from wood, Biomacromolecules 8 (2007) 3276–3278, https://doi.org/10.1021/bm700624p.

[8] X. Yang, M.S. Reid, P. Olsén, L.A. Berglund, Eco-friendly cellulose nanofibrils designed by nature: effects from preserving native state, ACS Nano 14 (2020) 724–735, https://doi.org/10.1021/acsnano.9b07659.

[9] M. Nogi, S. Iwamoto, A.N. Nakagaito, H. Yano, Optically transparent nanofiber paper, Adv. Mater. 21 (2009) 1595–1598, https://doi.org/10.1002/adma.200803174.

[10] H. Fukuzumi, T. Saito, T. Iwata, Y. Kumamoto, A. Isogai, Transparent and high gas barrier films of cellulose nanofibers prepared by TEMPO-mediated oxidation, Biomacromolecules 10 (2009) 162–165, https://doi.org/10.1021/bm801065u.

[11] J. Nemoto, T. Saito, A. Isogai, Simple freeze-drying procedure for producing nanocellulose aerogel-containing, high-performance air filters, ACS Appl. Mater. Interfaces 7 (2015) 19809–19815, https://doi.org/10.1021/acsami.5b05841.

[12] T. Benselfelt, J. Shakya, P. Rothemund, S.B. Lindström, A. Piper, T.E. Winkler, A. Hajian, L. Wågberg, C. Keplinger, M.M. Hamedi, Electrochemically controlled hydrogels with electrotunable permeability and uniaxial actuation, Adv. Mater. 35 (2023) e2303255, https://doi.org/10.1002/adma.202303255.

[13] S. Fujisawa, E. Togawa, K. Kuroda, Facile route to transparent, strong, and thermally stable nanocellulose/polymer nanocomposites from an aqueous Pickering emulsion, Biomacromolecules 18 (2017) 266–271, https://doi.org/10.1021/acs.biomac.6b01615.

[14] S. Sinquefield, P.N. Ciesielski, K. Li, D.J. Gardner, S. Ozcan, Nanocellulose dewatering and drying: current state and future perspectives, ACS Sustain. Chem. Eng. 8 (2020) 9601–9615, https://doi.org/10.1021/acssuschemeng.0c01797.

[15] C. Li, T. Kasuga, K. Uetani, H. Koga, M. Nogi, High-speed fabrication of clear transparent cellulose nanopaper by applying humidity-controlled multi-stage drying method, Nanomaterials (Basel). 10 (2020) 2194, https://doi.org/10.3390/nano10112194.

[16] V. Guccini, S. Yu, M. Agthe, K. Gordeyeva, Y. Trushkina, A. Fall, C. Schütz, G. Salazar-Alvarez, Inducing nematic ordering of cellulose nanofibers using osmotic dehydration, Nanoscale 10 (2018) 23157–23163, https://doi.org/10.1039/c8nr08194h.

[17] J. Sheng, R. Yang, A facile method to concentrate cellulose nanofibril slurries, Cellulose 26 (2019) 679–682, https://doi.org/10.1007/s10570-018-2099-2.

[18] Y. Sekine, T. Nankawa, S. Yunoki, T. Sugita, H. Nakagawa, T. Yamada, Eco-friendly carboxymethyl cellulose nanofiber hydrogels prepared via freeze cross-linking and their applications, ACS Appl. Polym. Mater. 2 (2020) 5482–5491, https://doi.org/10.1021/acsapm.0c00831.

[19] H. Kim, B. Endrődi, G. Salazar-Alvarez, A. Cornell, One-step electro-precipitation of nanocellulose hydrogels on conducting substrates and its possible applications: coatings, composites, and energy devices, ACS Sustain. Chem. Eng. 7 (2019) 19415–19425, https://doi.org/10.1021/acssuschemeng.9b04171.

[20] X. Guo, H. Gao, J. Zhang, L. Zhang, X. Shi, Y. Du, One-step electrochemically induced counterion exchange to construct free-standing carboxylated cellulose nanofiber/metal composite hydrogels, Carbohydr. Polym. 254 (2021) 117464, https://doi.org/10.1016/j.carbpol.2020.117464.

[21] T. Kasuga, H. Yagyu, K. Uetani, H. Koga, M. Nogi, Cellulose nanofiber coatings on cu electrodes for cohesive protection against water-induced short-circuit failures, ACS Appl. Nano Mater. 4 (2021) 3861–3868, https://doi.org/10.1021/acsanm.1c00267.

[22] T. Kasuga, T. Saito, H. Koga, M. Nogi, One-pot hierarchical structuring of nanocellulose by electrophoretic deposition, ACS Nano 16 (2022) 18390–18397, https://doi.org/10.1021/acsnano.2c06392.

[23] T. Kasuga, C. Li, A. Mizui, S. Ishioka, H. Koga, M. Nogi, Electrodeposition of cellulose nanofibers as an efficient dehydration method, Carbohydr. Polym. 340 (2024) 122310, https://doi.org/10.1016/j.carbpol.2024.122310.

[24] M. Citeau, O. Larue, E. Vorobiev, Influence of salt, pH and polyelectrolyte on the pressure electro-dewatering of sewage sludge, Water Res. 45 (2011) 2167–2180, https://doi.org/10.1016/j.watres.2011.01.001.

[25] L. Martin, V. Alizadeh, J. Meegoda, Electro-osmosis treatment techniques and their effect on dewatering of soils, sediments, and sludge: a review, Soils Found. 59 (2019) 407–418, https://doi.org/10.1016/j.sandf.2018.12.015.

[26] J. Wetterling, K. Sahlin, T. Mattsson, G. Westman, H. Theliander, Electroosmotic dewatering of cellulose nanocrystals, Cellulose 25 (2018) 2321–2329, https://doi.org/10.1007/s10570-018-1733-3.

[27] K. Nishio, H. Masuda, Anodization of gold in oxalate solution to form a Nanoporous black film, Angew. Chem. Int. Ed. 50 (2011) 1603–1607, https://doi.org/10.1002/ANIE.201005700.

[28] Y. Nishina, Mass production of graphene oxide beyond the laboratory: bridging the gap between academic research and industry, ACS Nano (2024), https://doi.org/10.1021/acsnano.4c13297.

[29] M. Zhao, F. Ansari, M. Takeuchi, M. Shimizu, T. Saito, L.A. Berglund, A. Isogai, Nematic structuring of transparent and multifunctional nanocellulose papers, Nanoscale Horiz. 3 (2018) 28–34, https://doi.org/10.1039/c7nh00104e.

[30] T. Saito, T. Uematsu, S. Kimura, T. Enomae, A. Isogai, Self-aligned integration of native cellulose nanofibrils towards producing diverse bulk materials, Soft Matter 7 (2011) 8804–8809, https://doi.org/10.1039/C1SM06050C.

[31] A. Sone, T. Saito, A. Isogai, Preparation of aqueous dispersions of TEMPO-oxidized cellulose nanofibrils with various metal counterions and their super deodorant performances, ACS Macro Lett. 5 (2016) 1402–1405, https://doi.org/10.1021/acsmacrolett.6b00786.

[32] A. Isogai, T. Saito, H. Fukuzumi, TEMPO-oxidized cellulose nanofibers, Nanoscale 3 (2011) 71–85, https://doi.org/10.1039/c0nr00583e.

[33] M.C. Hsieh, H. Koga, K. Suganuma, M. Nogi, Hazy transparent cellulose nanopaper, Sci. Rep. 7 (2017) 41590, https://doi.org/10.1038/srep41590.

[34] N. Isobe, T. Kasuga, M. Nogi, Clear transparent cellulose nanopaper prepared from a concentrated dispersion by high-humidity drying, RSC Adv. 8 (2018) 1833–1837, https://doi.org/10.1039/c7ra12672g.

[35] T. Kasuga, N. Isobe, H. Yagyu, H. Koga, M. Nogi, Clearly transparent nanopaper from highly concentrated cellulose nanofiber dispersion using dilution and sonication, Nanomaterials (Basel). 8 (2018) 104, https://doi.org/10.3390/nano8020104.

[36] K.M.O. Håkansson, I.C. Henriksson, C.D.L.P. Vázquez, V. Kuzmenko, K. Markstedt, P. Enoksson, P. Gatenholm, Solidification of 3D printed nanofibril hydrogels into functional 3D cellulose structures, Adv. Mater. Technol. 1 (2016) 1600096, https://doi.org/10.1002/admt.201600096.

[37] V. Klar, J. Pere, T. Turpeinen, P. Kärki, H. Orelma, P. Kuosmanen, Shape fidelity and structure of 3D printed high consistency nanocellulose, Sci. Rep. 9 (2019) 3822, https://doi.org/10.1038/s41598-019-40469-x.

[38] S. Ishioka, N. Isobe, T. Hirano, N. Matoba, S. Fujisawa, T. Saito, Fully wood-based transparent plates with high strength, flame self-extinction, and anisotropic thermal conduction, ACS Sustain. Chem. Eng. 11 (2023) 2440–2448, https://doi.org/10.1021/acssuschemeng.2c06344.

[39] S. Ishioka, T. Hirano, N. Matoba, N. Isobe, S. Fujisawa, T. Saito, Property-thickness correlations of transparent all-nanocellulose laminates, J. Fiber Sci. Technol. 79 (2023) 156–164, https://doi.org/10.2115/FIBERST.2023-0020.

[40] K. Daicho, K. Kobayashi, S. Fujisawa, T. Saito, Crystallinity-independent yet modification-dependent true density of Nanocellulose, Biomacromolecules 21 (2020) 939–945, https://doi.org/10.1021/acs.biomac.9b01584.

[41] K. Daicho, K. Kobayashi, S. Fujisawa, T. Saito, Recovery of the irreversible crystallinity of Nanocellulose by crystallite fusion: a strategy for achieving efficient energy transfers in sustainable biopolymer skeletons, Angew. Chem. Int. Ed. 60 (2021) 24630–24636, https://doi.org/10.1002/ANIE.202110032.

[42] H. Yagyu, T. Kasuga, N. Ogata, H. Koga, K. Daicho, Y. Goi, M. Nogi, H. Yagyu, T. Kasuga, N. Ogata, H. Koga, M. Nogi, K. Daicho, Y. Goi, Evaporative dry powders derived from cellulose nanofiber Organogels to fully recover inherent high viscosity and high transparency of water dispersion, Macromol. Rapid Commun. 44 (2023) 2300186, https://doi.org/10.1002/MARC.202300186.